

Dark Matter Genesis

JEREMY MOULD^{1,2}

¹*Swinburne University*

²*ARC Centre of Excellence for Dark Matter Particle Physics*

(Received Nov 3 2024; Revised Dec 2, 2024; Accepted Dec 30, 2024)

ABSTRACT

Recent discoveries of primordial black hole (PBH) candidates by means of high cadence microlensing open the way to a physical understanding of the formation of dark matter as a chapter in the thermal history of the Universe. Two complementary sites of PBH formation are considered, inflation and the early Universe at TeV to MeV energies. In the latter case the Friedman equation, together with mass measurements, reveal the threshold energy, the mass spectrum and the likely end point of this epoch. Some of the many recent exoplanet detections may conceivably have been detections of PBHs. When the Universe cools to MeV temperatures, larger mass PBH would form similarly, reaching the supermassive regime. The discovery of numerous supermassive black holes (SMBH) at high redshift with JWST fulfils this expectation. We corroborate the idea that Planck mass relics could be an important component of dark matter, and find that these are formed by PBH with initial mass less than approximately $6 \times 10^{-16} M_{\odot}$ and cosmic temperature above 10^9 GeV. Although in some mass ranges PBH can only make up a modest fraction of Ω_{matter} , it is possible that all astrophysical dark matter, as distinct from axions and WIMPs, is of PBH origin.

Keywords: Primordial black holes(1292) – Cosmology(343) – Gravitational microlensing exoplanet detection(2147) – Inflationary universe(784) – Supermassive black holes (1663)

1. INTRODUCTION

Gravitational microlensing was first to show that at least 80% of galaxies' mass is non-baryonic (Alcock et al. 1998, Silk 2000), and this has been confirmed and strengthened by observations of the microwave background. Following the possible discovery by Niikura et al. (2019) of a primordial black hole (PBH) with a mass in the range 10^{-11} to 10^{-6} solar masses and others at the high end of this range, we consider how such objects may be formed and evolve. PBHs have long been associated with the initial period of inflation that drove exponential expansion of the universe (Byrnes & Cole 2021). Here we propose that these seeds grew during the radiation dominated era §3, and we follow their evolution to the present day, through recombination, the surface of last scattering of the remaining photons, to galaxy formation (§4) to the properties of survivors today (§5). We raise the possibility in §5 that some exoplanet discoveries may have been misclassifications of PBH. Our conclusions in §6 include a proposed test for the PBH fraction of dark matter via rotation curve measures of M^* galaxies at $z = 1$. Forthcoming new facilities for microlensing will advance this probe of the early universe.

2. PRIMORDIAL BLACK HOLES AS DARK MATTER

PBHs meet the basic criteria for a good dark matter candidate. They are cold, non-baryonic and stable, but they are not totally dark, radiating with a temperature inversely proportional to their mass, so long as they remain above the Planck mass. Zel'dovich and Novikov (1967) and Hawking (1971) found that PBHs could form from overdensities in the early Universe. If they form before nucleosynthesis, PBHs are non-baryonic. Recent reviews are by Green (2024) and Carr & Kuhnel (2022).

In the Carr & Hawking (1974) collapse model, the PBH mass M can be related to the horizon mass at the time of its formation, $M = \kappa M_H$, where $M_H = c^3/(2GH)$ is the horizon mass, and κ is the efficiency of collapse. From the conservation of entropy in the adiabatic cosmic expansion, Carr et al. (2021b) find $M \approx 10^{15} (0.05/k_{PBH})^2 M_{\odot}$, where k is wavenumber in Mpc^{-1} and $k = aH/c$, with $H = \dot{a}/a$ and a the scale factor, H being close to constant to drive exponential expansion. Gouttenoire & Volansky (2024) find solar mass PBH in supercooled phase transitions at TeV temperatures. There are many proposals for PBH formation during inflation covering a range in k as broad as the different potentials under consideration. Here we shall be agnostic about this, as we suppose that PBHs formed during inflation are simply the seeds for density peaks present during the following radi-

ation dominated era. A timeline for this hybrid approach to PBH formation is shown by Ai, Heurtier & Jung (2024, their Figure 2).

3. PHYSICAL CONDITIONS AT DMG

The Friedman equation for a radiation dominated Universe, expressed in terms of the Schwarzschild radius of the PBH is $r = ct/8$, where t is the time since the Big Bang. This yields a time of formation for a $10^{-7} M_{\odot}$ object of 10 femtosec. At this time the cosmic temperature was 11 TeV. Lu et al. (2023) have proposed models in this energy regime for 10^{-5} , 10^{-9} and $10^{-12} M_{\odot}$ PBHs. They invoke beyond the standard model (BSM) physics as the trigger at these energies.

Karam et al. (2023) make models in which high amplitude curvature perturbations lead to the formation of PBHs. These cover a range of wavenumbers k from 10^{13} to $5 \times 10^6 Mpc^{-1}$ and PBH masses from 5×10^{-14} to $0.5 M_{\odot}$. The abundance of PBH is a strong function of the peak amplitude, and for a wide range of the PBH masses we are concerned with here, it seems possible to have Ω_{PBH} approach unity by choosing the peak amplitude. The shape of the mass spectrum is $\sim M^4 e^{-7M/2}$, but this may result from the choice of the Press-Schechter (1974) formalism.

As an alternative to Press-Schechter (PS) we propose a geometric formalism. PS asks what is the likely spectrum of density peaks? Instead, we ask, once a large spherical PBH has formed, how many smaller ones can be fitted around it? That said, we cannot neglect that the physics of these density peaks is unclear. The QCD phase transition has been advanced as a possible site (e.g. Musco, Jedamzik & Young 2024; Carr et al. 2021a), as the short range nuclear strong force suddenly yields to the cosmic expansion. In addition to this problem, there is the question of how PBH of any mass have avoided leaving a signature on Big Bang Nucleosynthesis, noted first by Bicknell & Henriksen (1979).

3.1. PBH initial mass function

Assuming that PBHs actually are a significant fraction of galaxies' dark matter, packing theory¹ can be applied, with PBHs forming in random parts of the volume that we nominally call overdensities, although we do not track density fluctuations in this toy model, the only condition being that they do not overlap. Packing theory quantifies the notion that in a given space more small objects will fit than large objects as, $N = 1 - \ln f$ where f is the fractional area/volume/radius, independent of dimensionality², and with $f < 1$, then $N > 1$. For scale factor $a \sim \sqrt{t}$ in the radiation era, and $a \sim e^t - 1 \approx t$ for small t in inflation. In the latter case $\log N + \log t = \text{constant}$ and $\log N + \log M = \text{constant}$. For $a \sim \sqrt{t}$ in the radi-

ation era (RE), $2 \log N + \log M = \text{constant}$. Both power law IMFs are shown in Figure 1. Measuring the mass function of PBHs can tell us whether a PBH burst was seeded during inflation or wholly the progeny of the RE. Carr & Silk (2016) recommend a power law IMF for PBH.

The packing process stops when it is impossible to fit any more of the steadily larger PBHs demanded by $r \sim t$ in the co-moving volume. Figure 1 shows the $(\log N, \log M)$ mass distribution that results. The masses have been normalized so that the most likely mass is equated to the high end of the Subaru team mass range. This identifies the time scale of the formation process and the temperature of the Universe during that time. Without it, there is nothing in the toy model but dimensionless radii, which are proportional to the mass, and thus normalizable to it.

The peak and rapid fall of the mass distribution means that it was most likely that the first PBH microlens to be detected would be close to the maximum mass to form, even though the new high cadence experiment, in contrast to earlier work (Alcock et al. 1993; Paczynski et al. 1996), was sensitive to lower masses. This makes normalization to the very first PBH to be announced as such less hazardous than if the $(\log N, \log M)$ distribution were flat.

Since $r \sim M \sim t$, once the formation process has started, progressively larger PBHs are formed, steadily filling the Universe. The matter that is not subsumed into PBHs is free to move on to the next stages in the thermal history of the Universe, baryogenesis and primordial nucleosynthesis, which occurs one second later. In what follows we consider PBH dark matter to be a significant part of galaxy halo dark matter. It is not necessary that it be dominant, and it can co-exist with non-baryonic particle dark matter. The fraction of dark matter in the mass range we discuss that is PBH can be determined by high cadence microlensing experiments. We emphasize that both PS and packing theory are formalisms rather than strict physical theories. We see them as alternatives and even complementary. Mould & Batten (2024) show that the packing theory IMF leads to an excellent fit of the QSO luminosity function, if the supermassive black hole (SMBH) nuclei are large PBH.

3.2. Other formation theories

Carr et al. (2019) favor a multi-modal PBH mass spectrum with peaks at 10^{-6} , 1, 30, and $10^6 M_{\odot}$. This suggests a unified PBH scenario which naturally explains the dark matter and recent microlensing observations, and the origin of the SMBH in galactic nuclei at high redshift. By comparison the models of Lu et al. are also peaked at the energies where they assume a phase transition, except for the lowest mass model ($10^{-12} M_{\odot}$) which is broader and rises to lower masses. They draw on the PS formalism, and find the PBH fraction of the dark matter to be 100% in their lowest mass case, 0.5% in the 10^{-9} case and 2% in the highest mass case. The latter two cases would be hard to detect in microlensing experiments, as the event rate towards the LMC $\sim 1.6 \times 10^{-6} \sqrt{(M_{\odot}/M)}$ per year for a 100% PBH Galactic halo (Moniez 2001). The lowest mass is a problem observation-

¹ <https://www.vedantu.com/chemistry/unit-cell-packing-efficiency>

² For example, for area, $dn = (A_0 - A(f))/fA_0 = -df/f$. Apply that to two values of the scale factor a , $a+da$: $n(a) = 1 - \ln f(a)$ and $n(a+da) = 1 - \ln f(a+da)$. So $dn(a) = \ln(f(a+da)/f(a)) = \ln(da)$. Integrate from a_0 to a : $n(a) - n(a_0) = a \ln a - a_0 \ln a_0 + a_0$. Suppose $a = a_0 x$; $a_0 = a/x$; then $N = n(a) - n(a_0) = \ln x - a$. For $N \gg \ln x$, $\log N = -\log a + \text{constant}$.

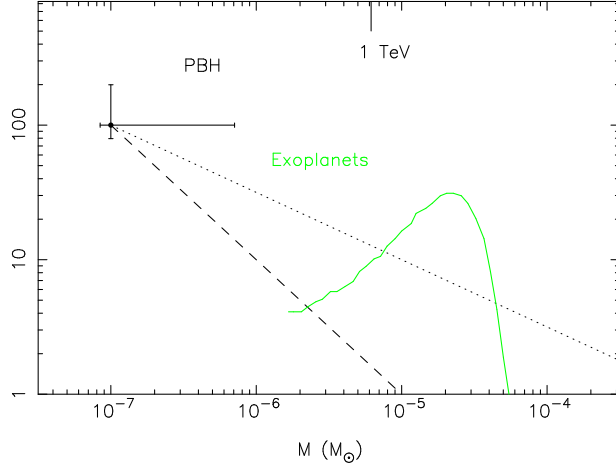


Figure 1. On the low mass side the mass distribution (IMF) is of the form $\log N + \log M = \text{constant}$, illustrated by the dashed line. There is a sharp cutoff on the low mass side where the PBH with the largest Schwarzschild radius is the first mass to be accommodated. A second IMF $2\log N + \log M = \text{constant}$ is the dotted line. The limitations of this toy model are outlined in §3.3. The point at $10^{-7} M_{\odot}$ is close to an IMF peak proposed by Carr et al. (2019). The green dashed curve is a *Kepler* exoplanet mass function from Suzuki et al. (2016). In §5.2 we ask whether any PBH microlensing events have been misclassified as exoplanets. If this happened to be the shape of the curve of a PBH mass function, it could be the signature of a burst of PBH formation later than that shown. As the mass axis is also a cosmic cooling axis, an energy of a TeV is marked.

ally because of finite source effects. That is to say, the Einstein radius has become so small that an amplification event has begun to turn into a transit. An alternative to PS is peak theory in which the number density is calculated of peaks where compact objects like galaxies and PBHs are expected to form, if the density contrast exceeds some threshold (Wang et al. 2021). With 10^{-13} and $30 M_{\odot}$ models they achieve 2 or 3 orders of magnitude higher PBH production,

3.3. Lessons from the toy model

What packing theory fails to predict accurately is the fraction of mass in the Universe that is PBH dark matter. Assuming random relative positioning of PBHs, the packing fraction is expected to be 64%, whereas what is observed for the sum of all species of non-baryonic dark matter is 81% (Ade et al. 2020). A physical model would trigger PBH formation at density inhomogeneities and could make a successful prediction of a high dark matter fraction. Nevertheless, the geometric toy model motivates the investigation of that physics and strongly suggests that it is the finite radius and stability of black holes that determines how many baryons remain in the Universe to go on to make nuclei, atoms, galaxies and us.

Everything we see around us may be just the leftovers from the primordial black holes which attempted to consume most of the Universe in its first seconds, were involved in seeding SMBH during primordial nucleosynthesis, hosted and controlled³ galaxy formation when cosmic temperatures had cooled sufficiently, and are still around maintaining galaxies today.

To sum up, the Friedman equation for the radiation dominated era is prescriptive, but insufficient. At any time t in this energy range there is a specific radius of PBH that *can* be formed, $r = ct/8$. Whether a PBH *does* form at that time involves TeV physics, possible seeding during inflation, and density inhomogeneity, as well as geometry.

4. PBH EVOLUTION

PBH evaporate with age as $kT = \hbar c/4\pi r$ (Hawking 1971). Evolutionary tracks are shown in Figure 2 for a number of different masses. As the universe ages according to the Friedman equation through its radiation, matter and dark energy dominated stages, the PBH sticks to its Hawking equation. We used the mass loss rates of Mosbech & Picker (2022) to evolve ten different masses between 10^{-23} and $10^{-1} M_{\odot}$. A dimensionless mass loss rate $d\log M/d\log t$ is more suitable to our $d\log kT$ time steps. For reference, $d\log M/d\log t \approx -1$ for main sequence stars, their luminosity being $c^2 dM/dt$, where dM is the mass loss due to fusion. Intermediate mass PBH have $d\log M/d\log t = -13.16 \alpha_{24} (m_{20})^{-3} (kT)^{-2}$, where kT is the cosmic temperature in eV (the x-axis in Figure 2) and m_{20} is the mass in $10^{-20} M_{\odot}$ units. For $\log M / M_{\odot} > -15.3$, $\alpha_{24} = 1$, and for smaller PBH Mosbech & Picker give a fit to it. While the above relation is strictly for RE, similar expressions can be written for the matter and dark energy dominated universe.

The lowest mass PBH do not reach matter/radiation equality before evaporating off the plot.

4.1. Recombination

For any temperature of the Universe there is an mn PBH that is evaporating at that time. The track becomes almost vertical at that kT . And this is true for $kT = 13.6$ eV for a PBH mass of m_{20} . The duration of recombination is approximately from $13.6/kT-1$ to $13.6/kT+1$. That neglects electron density n_e and $T^{3/2}$ which shorten the time a bit, as n_e decreases as the scale factor a increases. The extent of δT is $d\ln T = 2k/13.6 = d\ln(1+z) = d\ln t / 2$ for the RE. It is easy to show⁴ $d\log M/d\log t = 7/3$ at the half mass point of a PBH. So the mass range evaporating during recombination is $\delta \ln M = 17.2/13.6 \cdot 14/3 \cdot 10^{-5}$.

PBH ionise their environment when they evaporate to $x=0.19$, the baryonic mass fraction, where x is the degree of

³ By "controlled" we mean that mass losing PBH can provide the feedback mechanism that calls time on galaxy collapse.

⁴ For PBH initial mass M_0 and a constant k , $dM/dt = -k/M^2$ and $d\ln M/d\ln t = -kt/M^3$. Integrate: $dM/M^2 = -kdt$, to get $(M_0^3 - M^3) = 3kt$. Divide: $3d\ln M/d\ln t = (M_0/M)^3 - 1$. So $d\ln M/d\ln t$ starts at zero, and at its half mass time is $7/3$. It continues to rise.....

ionisation. So put $13.6/\delta(kT) = 0.19$, the temperature change required to compensate for PBH ionisation. That is $13.6 \ln kT = 0.19$ or $d \log kT = 0.006$, barely visible on our tracks. Or $\delta \log t \approx 0.01$. And that is also the change in the age of the Universe and H_0 , 2.3%. An exact treatment of recombination with PBH evaporation is warranted Seager, Sasselov & Scott 1999, Slatyer 2015, Batten & Mould 2024).

This delay of recombination is analogous to some of the varied solutions to the Hubble tension considered by di Valentino & Silk (2023). Although PBH are mentioned in their review, the ionization time bomb mechanism described here is different. Scars that might be left on the surface of last scattering also need examination.

4.2. Matter domination

The next transition for larger PBH is the end of the RE at $z \approx 3400$ in the Planck cosmology (Ade et al. 2020), which we use throughout. The second is crossing the surface of last scattering of the cosmic microwave background (CMB). Next is redshift 100, close to the free fall time for galaxies, which moves left or right depending weakly on the mass under consideration. Low mass PBH reach that line (together with accompanying WIMPs) to form dark matter halos into which the baryons will fall. Finally, the start of the dark energy epoch is defined by $a_{DE}^3 = \Omega_m/\Omega_\Lambda = 0.43$. From the start of matter domination (MD) to the onset of

We adopt a nomenclature for PBH in which m11 is a PBH of mass $10^{-11} M_\odot$ and M7 has $10^7 M_\odot$. We note that PBH smaller than m16.8 have now reached Planck mass, $m_P = 22 \mu\text{g}$. Profumo (2024) discusses whether PBH stall at m_P or continue on to lower masses⁵. If PeV physics and beyond permits them to be made, they could number up to 10^{50} in the Galaxy (see also MacGibbon 1987 and Taylor et al. 2024). At 10^{-20} the radius of the proton, these objects would pass through ordinary matter, if geometric cross sections are a guide. Planck mass relics have an area of 10^{-65}cm^2 , and the reaction rate with gas per unit volume would be below 10^{-10} per year. Such relics in the Milky Way might contribute to the cosmic ray rate, but at $22 \mu\text{g}$ are ultrarare and 10^{10} times more energetic than the OMG CR observed in 2021. As non-baryons their interaction with normal matter is outside the scope of this paper, but in a sense they might be regarded as fundamental particles with a macroscopic mass, and could even be described as ultramassive WIMPs.

The dependence of the morphology of Figure 2 on fundamental constants is interesting. The Boltzmann constant zeropoints both axes equally. The Planck constant controls the rate of cooling of the PBH. Newton's constant controls the time/temperature x-axis. To the left of the radiation to matter transition that is all there is. Ω_{matter} affects the slope thereafter, but §3.1 hypothesises that Ω_{matter} is determined by something as simple as packing geometry.

⁵ An $h\nu = kT$ photon at the Hawking temperature has an energy of $200 m_P$, seemingly a hard task for a Planck mass particle to emit.

4.3. Galaxy formation

From the end of RE at t_{eq} there is an infall radius of matter for a PBH of mass M of $gt^2/2$, with $gt \ll c$, where t is the time since the end of RE and g is the gravitational acceleration into the PBH, and (until galaxy formation) a corresponding infall. These infall regions can attain kpc size in Myrs, making them protogalaxy candidates. Closer to the PBH itself, a photosphere would attain hydrostatic equilibrium with pressure $P = g m_e/\sigma_e$, where these quantities are the mass and Thomson cross section of the electron. $P = 1.5 \times 10^{-4} g$ and $g = c^4/GM = 6 \times 10^{17}/M \text{cm s}^{-2}$ with M in solar units. This would slow the timescale for mass loss to a diffusion time, as is the case for conventional stars. Radiative transfer in a relativistic infalling gas is beyond the scope of this paper, but for masses larger than the subsolar range in figure 2, is important to explore in the context of protogalactic nuclei. After galaxy formation the density of matter surrounding a PBH drops to that of the intergalactic medium (IGM), which, for $\rho_{IGM} \ll \rho_{galaxies}$, is insufficient to sustain infall.

Like other forms of dark matter, at $\sim 10^8$ years PBH collapse into a potential well of their own making. PBH that lose mass in the galaxy formation period (30, 3) in redshift have a small range in mass between $m_1 \sim m17$ and $m_2 \sim m19$. For PBH the mass loss is $d \log M/d \log t = \sim -(kT_{PBH}/10 \text{ GeV})^3$, a runaway rate. We carried out a test with a 100,000 particle scale free dark-matter-only n-body simulation. Similar structures resulted in both the mass losing and the mass conserving case. A 3% increase in the circular velocity of the resultant potential resulted from a 12% loss in total mass. Effectively, mass losing PBH are providing feedback, often attributed to mechanisms not intrinsic to the collapse process.

4.4. Matter density stability

If PBH are a significant fraction of the dark matter and they lose mass, how come Ω_m measured in the cosmic microwave background (CMB) $\approx \Omega_m$ now? The answer may be in the mass range that has lost mass between passing the redshift of the surface of last scattering and the current time. The range is m15.2 to m19.2, and those PBH would have lost essentially 100% of their mass in that period. We have no observational data on that mass range, only broadly on the range m11 to m6 which are too large to evaporate, as $dM/dt \sim M^{-2}$. In the range that has lost mass since the CMB redshift the limit on Ω_m is an integral over the PBH mass range, m1 to m2

$$\begin{aligned} \frac{\Delta \Omega_m}{\Omega_m} &= 1.75 f \int_{m1}^{m2} dm \frac{2 \ln 10}{m1 + m2} = 1.75 f \ln 10 \frac{m2 - m1}{m1 + m2} \\ &= 1.75 f \ln 10 \end{aligned}$$

The uncertainty in Ω_m found by Davis et al. (2024) in the Dark Energy Survey then requires $1.75 f \ln 10 < 0.017/0.27$ and $f \lesssim 1.5\%$ for a flat, constant equation of state cosmology. The limit becomes 7.5% in a variable w (equation of state) cosmology. This can be relaxed (Efstathiou 2024) by

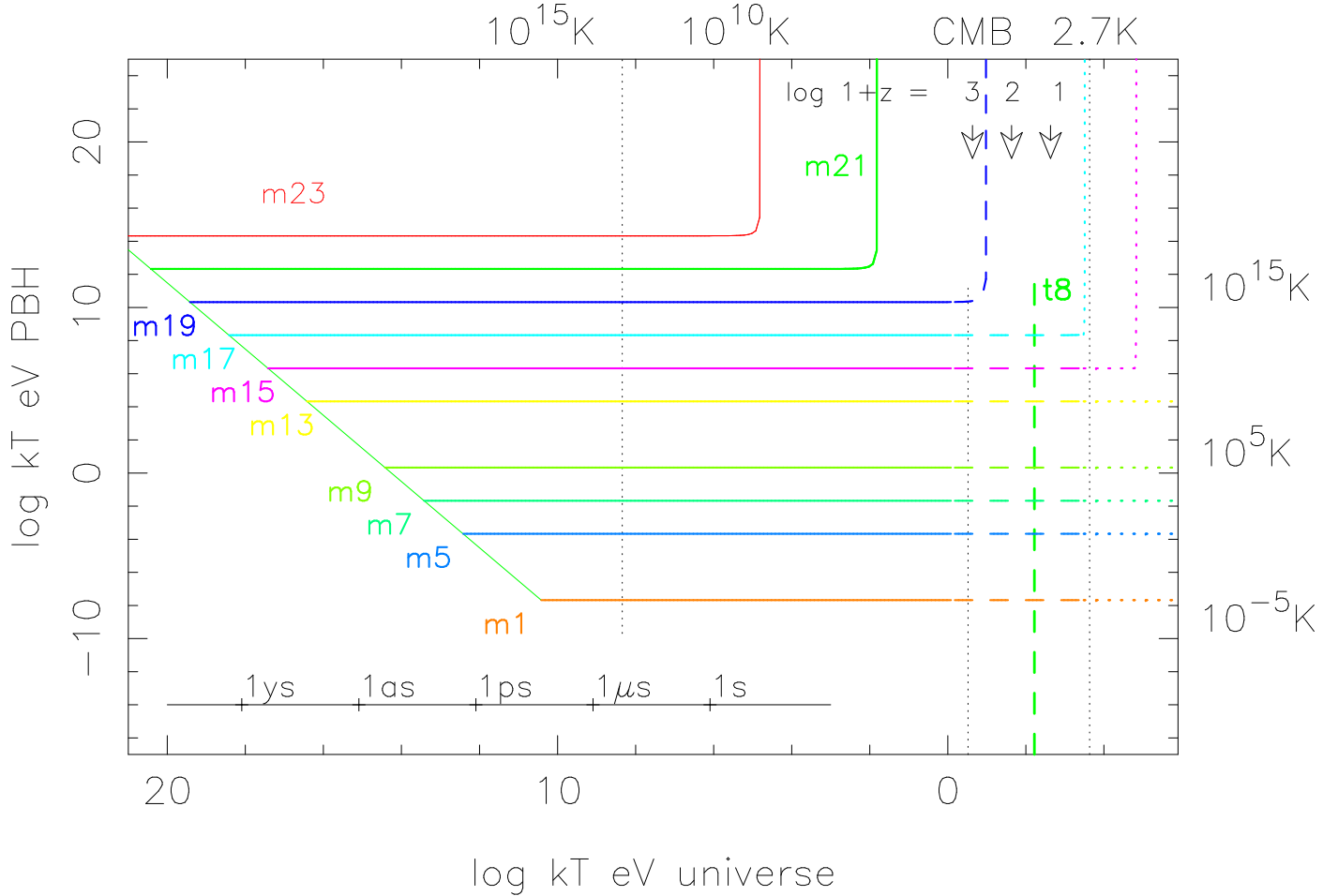


Figure 2. Evolution of 10 different mass PBH in PBH temperature vs cosmic temperature. Kelvin units are on the top and right borders. PBH changing their evolutionary rate as $T \sim M^{-1}$, from radiation (solid line), to matter (dashed line), to dark energy dominated (dotted line). The t8 line marks the start of galaxy formation. The three dotted vertical lines are from left to right the QCD transition at 220 MeV, the surface of last scattering of the CMB and the temperature today, 2.7K. The first of these is discussed as a possible PBH trigger by Alonso-Monsalve & Kaiser (2023). As the universe cools, the lowest mass PBH take a right angle turn to high temperatures, rapidly becoming Planck mass relics.

allowing a 3% variation of the SNIa standard candle⁶. The conserved majority share of Ω_m would be a combination of PBH outside the m15 to m19 mass range, WIMPs and axions. Micro-PBH, which reach Planck mass before they come to the CMB line in Figure 2 may be an important contributor with a maximum initial mass $\approx 8 \times 10^{-20} M_\odot$.

4.5. The bandwidth of the PBH IMF

Finite source effects reduce the optical depth in the LMC line of sight for low mass PBH. A further, but speculative, re-

duction may come about from the PBH IMF. If every decade in mass has equal mass ($n \sim m^{-1}$), and a given microlensing experiment is sensitive to 2 decades in cadence, then only 4 decades in mass from the range m17 to M3 are covered, and the maximum PBH fraction of the dark matter, f , visible in that experiment is 20%. We chose m17, as that is the smallest mass that has not already fallen to the Planck mass. If PBH formation were to begin at the start of the RE at $\log kT \gtrsim 21$, $f < 10\%$ for an individual experiment. If the PBH IMF consists of discrete pieces, triggered by events in the RE, this limitation does not apply.

⁶ <https://www.issibern.ch/teams/shot/wp-content/uploads/sites/186/2024/07/issi.pdf>

The PBH IMF of Carr et al. (2019, their figure 2) shows one peak in the region of m6 PBH. These PBH should be detectable now.

5.1. The HR diagram for compact objects

Luminosities for PBHs were calculated from their radii and temperatures at the current epoch and are shown in Figure 3 together with the nearest white dwarfs and magnetars plus pulsars from the fundamental plane of Chu & Chang (2023). To eliminate the third parameter, we chose a typical 1.5 km radius. The m5 –m13 labels denote the initial and current masses of these objects. A close by m5 or m3 object would in principle be observable, The extraordinarily high temperatures predicted for PBH of lower mass than Figure 3 accommodates might not be possible for baryonic stars due to neutrino cooling. The bolometric correction for optical observers, moreover, for a very hot m13 PBH is of order 12.5 magnitudes. A further possible observational quirk of low mass PBH is that as they approach $10^{17} m_P$ (1.5 Mton), their radiation may become noticeably quantized to ~ 1 photon/second. There are objects in the Gaia DR3 archive at $1-10 \times 10^{-6} L/L_\odot$, but candidates will require spectroscopic sorting from brown dwarfs, which are surprisingly blue at Gaia wavelengths.

5.2. Have PBH been detected towards the Galactic center ?

Some of the 200 exoplanet detections (Mroz & Poleski 2024) in the line of sight to the Galactic bulge may have been PBHs, as the dark matter density peaks at the Galactic center. Based on optical depth calculations that fraction is approximately $30 \pm 5\%$ for a fully PBH halo and 3% for a 10% PBH halo. We discount possible Planck mass relics in this estimate. To calculate baryonic and non-baryonic τ , we used the Galaxy model by de Jong et al. (2010) but, to err on the side of caution, put a core on its NFW dark matter component, which otherwise has a cusp at the center of the Galaxy. Such cusps are not seen to last in galaxy evolution simulations. Adding a bulge from Binney & Vasiliev (2023), while supplying the source stars, made a very small change to the baryonic optical depth, because of its steep fall along the Baade’s Window line of sight to the observer, which was used for the calculations. Uncertainty about the behavior of the scale height of the disk (± 50 pc) at Galactic radii interior to the Sun’s imposes the nominal limits we have attached.

Figure 1 also shows a *Kepler* transit exoplanet mass function by Suzuki et al. (2016). Their M type primaries function was chosen, as these are the commonest stars in the Galaxy, but the G type function is similar with a somewhat higher peak mass and lower frequency of exoplanets per star. Both are consistent with microlensing exoplanet observations. We do not know if the early Universe made $10^{-5} M_\odot$ PBH, but if it did, their distribution function could fit within that curve. High cadence LMC microlensing would not have detected them, because the event rate from $10^{-5} M_\odot$ PBH would be a tenth that of the rate at $10^{-7} M_\odot$ (Moniez 2021). The combined Magellanic Cloud microlensing campaigns would have detected Jupiter mass PBHs, if they were present (Alcock

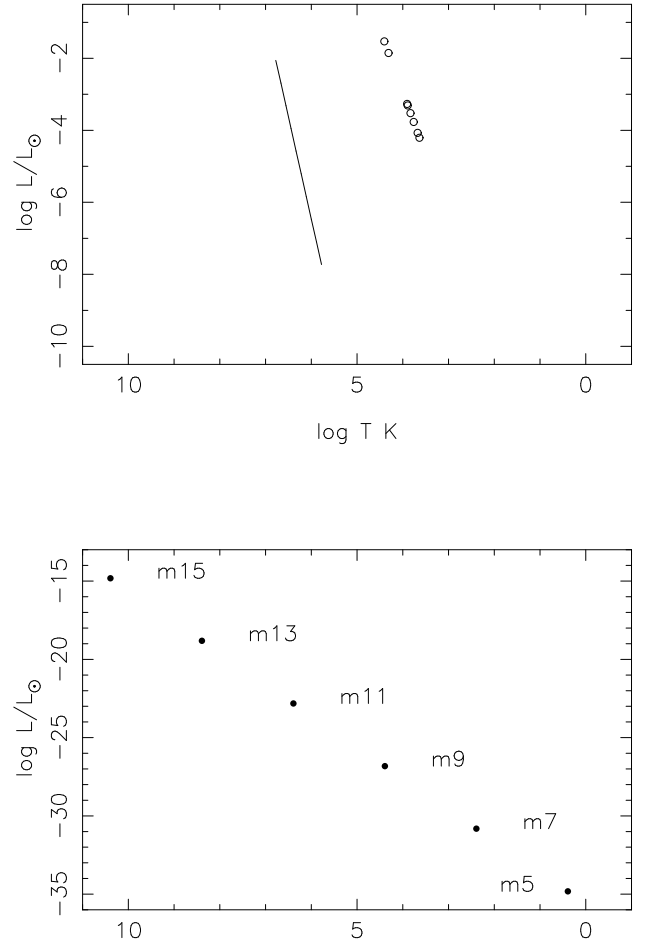


Figure 3. The Hertzsprung Russell diagram for PBHs of observable mass. Also shown is the nearby white dwarf cooling sequence (open circles) and pulsars plus magnetars from a linear fit by Chu & Chang (2023). The baryonic stellar remnants are cooling sequences. An m7 has a brown dwarf temperature. Pressure broadening at $\log g = 36$ would erase all spectral lines, however. PBH are the most compact of compact objects.

et al. 1998 ; Alfonso et al. 2003). Carr & Kuhnel (2022) and Alonso-Monsalve & Kaiser (2023) proposed the QCD phase transition at 220 MeV as a trigger for PBH formation. This would have produced $0.16 M_\odot$ M dwarfs, also not seen in LMC microlensing. The next significant energy level which the Universe passes through is 0.511 MeV. This corresponds to $1.4 \times 10^7 M_\odot$ PBH, or Supermassive PBH (Bicknell & Hendriksen 1979; Soltan 1982; Mould & Batten 2024), and Sobrinho & Augusto (2024) discuss this as an accompaniment to primordial nucleosynthesis. It is a possible

path for solution of the early SMBH problem identified by JWST (Labbé et al. (2024).

Sumi et al. (2023) fitted a Free Floating Planet (FFP) initial mass function to the results of the MOA 9 year microlensing survey (Koshimoto et al. 2023). The shortest Einstein time found in this survey was 0.057 days, twice the 0.0288 days for the $10^{-7} M_{\odot}$ Phoebe. The Einstein time $E_T \sim \sqrt{M}$, where M is the mass of the lens. Acceptable fits rise sharply at masses between 3×10^{-5} and $10^{-7} M_{\odot}$, depending on the parameters of the mass function. Microlensing FFPs can only be loosely defined as free floating, as they are required to show no underlying amplification of a host star with longer t_E in the light curve, a condition which can be found from simple analytical considerations to be satisfied by placing the planet beyond a Mars orbit for a $1 M_{\odot}$ host. Be that as it may, PBHs may masquerade as FFPs in their light curves, and the Sumi et al. mass distribution function may be occupied in part by PBHs at the level we have estimated from Baade's Window optical depths.

6. CONCLUSIONS

Setting aside the ambiguity of microlensing events from the Galactic bulge,

- the possible discovery of PBHs in the mass range 10^{-11} to $10^6 M_{\odot}$ places the formation of some of the dark matter as early as the quark epoch before baryogenesis at the electroweak scale (100 GeV), between the end of inflation and attoseconds after the Big Bang and as late as the primordial nucleosynthesis era.
- PBHs below $10^{-17} M_{\odot}$ would now be Planck mass relics and could account for a significant fraction of today's dark matter. These may have been seeded in a still earlier inflation scenario which seems capable of a wide range of formation predictions, both in mass and abundance ⁷
- Some of the exoplanet detections in the line of sight to the Galactic bulge may have been PBHs, as the dark matter density peaks at the Galactic center.
- Annihilation radiation from the Galactic center may be an associated dark matter signal (Song et al. 2024).
- Further observations to populate the mass spectrum and simulations that incorporate the physics of this energy domain, with geometrical distributions of PBHs other than uniform, are desirable to explore this chapter of the thermal history of the Universe fully. A sharp cuton could be evidence for the role of geometry as outlined here.

⁷ We could foresee in this scenario a particular PBH mass spectrum might point to a feature in the potential. Peaks in the power spectrum can be induced by a bump, dip or step in the potential (Karam et al. 2023).

- Results from supernova cosmology ($0.1 < z < 1$) and the CMB regarding the critical mass fraction in matter (Ω_m) suggest that only a modest percentage of the overall dark matter can be in the form of mass losing PBH with masses between m_{15} and m_{19} .
- The PBH era could seed the supermassive black holes that seem to be numerous at high redshift, if it extends to times of a few seconds (Mould & Batten 2024).
- Mass loss by m_{20} PBH could delay recombination, affecting the CMB H_0 .
- Dark matter halos with a fraction f of PBH in the range $m_{15.3}$ to $m_{17.3}$ may have lost that fraction of their mass to evaporation (to Planck mass relics) in the last 12.6 Gyr (i.e. since $z = 1$). Their $v^2 r$ should have been $100/f$ % larger than they are today, where v and r are the velocity and radius at the flat part of their rotation curves. Twenty one cm line width measurements of the Schechter function's M^* galaxies could test this prediction.
- Observations of the low mass end of the PBH spectrum below $10^{-8} M_{\odot}$, which can tell us more about the early Universe, are more difficult for Magellanic Cloud microlensing fields because of finite source star effects, which reduce the optical depth to lensing. But there is telescope construction underway that may meet the challenge (DeRocco et al. 2024).
- The cold dark matter paradigm is a minimalist theory, successful over almost fifty years. Additions are now being trialed, and the rich properties of PBH make them good candidates, even though their formation physics remains to be fully understood.

REFERENCES

- Ade, P. et al. , Planck collaboration 2020, A&A, 641, A6
 Ai, W-Y, Heurtier, L & Jung, T-H 2024, arxiv 2409.02175
 Alcock, C. et al. 1993, Nature, 365, 621
 Alcock, C. et al. 1998, ApJL, 499, L9
 Alfonso, C. et al. 2003, A&A, 400, 951
 Alonso-Monsalve, E. & Kaiser, D. 2023, Phys Rev L, 132.231402
 Batten, A. & Mould, J. 2024, in preparation
 Bicknell, G. & Henriksen, R. 1979, ApJ, 232, 670
 Binney, J. & Vasiliev, E. 2023, MNRAS, 520, 1832
 Byrnes, C. & Cole, P. 2021, arXiv 211205716
 Carr, B. et al. 2021a, PDU, 31, 00755
 Carr, B. et al. 2021b, RPPH, 84, 6902
 Carr, B. et al. 2019, Physics of the Dark Universe, 31, 755
 Carr, B. & Hawking, S. 1974, MNRAS, 168 399
 Carr, B. & Kuhnel, F. 2021, arxiv 21100282
 Carr, B. & Silk, J. 2016, MNRAS, 478, 3756
 Chu, C-Y & Chang, H-K 2023, MNRAS, 526, 1287
 Davis, T. et al. 2024, ApJ Letters in press
 de Jong, J. et al. 2010, ApJ, 714, 663

DeRocco, W. et al. 2024, PhRvD.109b3013
 Efsthathiou, G. 2024, arxiv 2408.07175
 Green, A. 2024, Nuclear Physics B, 1003, id.116494
 Gouttenoir, Y. & Volansky, T. 2024, arxiv 2305.04942
 Hawking, S., 1971, MNRAS, 152, 75
 Labbé, I. et al. 2024, Nature, 616, 266
 Koshimoto, N. et al. 2023, AJ, 166, 107
 Karam, A. et al. 2023, JCAP, 3, 13
 Lu, P. et al. 2023, Phys Rev Lett, 130, 1002
 MacGibbon, J. 1987, Nature, 329, 308
 Moniez, M. 2001, Proc. XXXVth Rencontres de Moriond,
 Tran, Mellier & Moniez. Les Ulis: EDP Sciences
 Mosbech, M & Picker, Z. 2022, SciPost, 13, 100
 Mould, J. & Batten, A. 2024, submitted to ApJL
 Mroz, P. & Poleski, R. 2024, Handbook of Exoplanets, 2nd
 Edition, Deeg and Belmonte (Eds), Springer
 Musco, I., Jedamzik, K. & Young, S. 2024, Phys Rev D. 109,
 3506
 Niikura, H. et al. 2019, Nature Astronomy, 3, 524
 Paczynski, B. et al. 1996, IAU Symposium, 169, 93
 Press, W. & Schechter, P. 1974, 187, 525
 Profumo, S. 2024, arxiv 2405.00561
 Rezaadeh, K. et al. 2022, EPJ C, 82, 8, id.758
 Seager, S., Sasselov, D. & Scott, M. 1999, ApJ, 523, L1
 Silk, J. 2000, Proc. 7th International Symposium on Particles,
 Strings and Cosmology, Eds: K. Cheung, & J. Guion
 Slatyer, T. 2015, arxiv 1506.03812
 Sobrinho, J. & Augusto, P. 2024, MNRAS, 531, L40
 Soltan, A. 1982, MNRAS, 200, 115
 Song, D. et al. 2024, MNRAS, 530, 4395
 Sumi, T. et al. 2023, AJ, 166, 108
 Suzuki, D. et al. 2016, ApJ, 833, 145
 Taylor, Q. et al. 2024, PhysRevD, 109, 406
 Wang, Q. et al. 2021, Phys Rev D, 104, 8, id.083546
 Zel'dovich, Y.B. & Novikov, I.D. 1967, Sov. Astron. 10, 602
 Zheng, R. et al. 2022, Chinese Physics C, 46, 4, id.045103

ACKNOWLEDGEMENTS

The ARC Centre of Excellence for Dark Matter Particle Physics is funded by the Australian Research Council. Grant CE200100008. Simulations were carried out on Swinburne University's Ozstar & Ngarrgu Tindebeek supercomputers, the latter named by Wurundjeri elders and translating as "Knowledge of the Void" in the local Woiwurrung language. I thank colleagues in our microlensing team and the CDMPP for helpful discussions and the referee for improvements to the paper.

CODE AVAILABILITY

The evolutionary tracks and toy model with README files are available at <https://github.com/jrmould> and [10.5281/zenodo.14195697](https://zenodo.org/record/14195697)

APPENDIX

The two equations assumed in §2 (and why $r = GM/c^2 \sim t$) are the Friedman equation for the radiation dominated era,

giving the energy density, to be multiplied by Hubble volume.

$$\frac{3}{32\pi G t^2} (tc)^3 4\pi/3 = M(\text{PBH})$$

and

$$t \approx 1.3 \left(\frac{1\text{MeV}}{kT} \right)^2 \text{ s} = 1.3 \left(\frac{1\text{GeV}}{kT} \right)^2 \mu\text{s} = 1.3 \left(\frac{1\text{TeV}}{kT} \right)^2 \text{ ps}$$

from radiation energy density $= 4\sigma T^4/c$ and the Friedman equation. Similarly for PeV and attoseconds. In inflation we have from Carr & Hawking

$$M/M_\odot = 1.13 \times 10^{15} \frac{\kappa}{0.2} \left(\frac{g^*}{106.75} \right)^{-1/6} \left(\frac{k^*}{k_{PBH}} \right)^2$$

where κ is efficiency of collapse, g^* is number of relativistic degrees of freedom and k_{PBH} is the wavenumber of the PBH as it exits the horizon and $k^* = 0.05 \text{ Mpc}^{-1}$.

The relationship between PBH initial mass and energy is $M/M_\odot = 3.3 \times 10^{-6} (1 \text{ TeV}/kT)^2$. The PBH range 5×10^{-7} to $5 \times 10^{-9} M_\odot$ is often called the PBH asteroid range (e.g. Caplan et al. 2023). In the temperature range, 100 down to 1 TeV, the Universe passed through the PBH initial mass range 3×10^{-10} to $3 \times 10^{-6} M_\odot$. Three cooling channels are available to it, expansion, PBH formation and endothermic particle reactions. So TeV physics will modulate the PBH production rate and thus the mass distribution function function in the observable range. Our toy model considered only geometry. Inhomogeneities and TeV physics, both LHC verified and BSM, would fill out the picture. An example is $g \Leftrightarrow \gamma\gamma$, where g is a gluon. This provides a rich field for astroparticle physicists and microlensing astronomers to interact in. To bridge the gap, astronomers could speak loosely of a 1 TeV PBH, to identify its origin in the early Universe.